ORIGINAL PAPER

Development of highly fluorescent silica nanoparticles chemically doped with organic dye for sensitive DNA microarray detection

Aihua Liu · Liyou Wu · Zhili He · Jizhong Zhou

Abstract Increasing the sensitivity in DNA microarray hybridization can significantly enhance the capability of microarray technology for a wide range of research and clinical diagnostic applications, especially for those with limited sample biomass. To address this issue, using reverse microemulsion method and surface chemistry, a novel class of homogenous, photostable, highly fluorescent streptavidin-functionalized silica nanoparticles was developed, in which Alexa Fluor 647 (AF647) molecules were covalently embedded. The coating of bovine serum albumin on the resultant fluorescent particles can greatly eliminate nonspecific background signal interference. The thus-synthesized fluorescent nanoparticles can specifically recognize biotin-labeled target DNA hybridized to the microarray via streptavidin–biotin interaction. The response of this DNA microarray technology exhibited a linear range within 0.2 to 10 pM complementary DNA and limit of detection of 0.1 pM, enhancing microarray hybridization sensitivity over tenfold. This promising technology may be potentially applied to other binding events such as specific interactions between proteins.

Keywords DNA microarray · Sensitivity · Silica nanoparticles chemically doped dye · Biotin–streptavidin interaction · Reverse microemulsion reaction

A. Liu · L. Wu (✉) · Z. He · J. Zhou (✉)
Institute for Environmental Genomics,
Department of Botany and Microbiology,
University of Oklahoma,
Norman, OK 73019, USA
e-mail: lwu@rccc.ou.edu
e-mail: jzhou@ou.edu

A. Liu (✉)
Qingdao Institute of Bioenergy & Bioprocess Technology,
and Key Laboratory of Bioenergy, Chinese Academy of Sciences,
189 Songling Road,
Qingdao, Shandong 266101, China
e-mail: liuah@qibebt.ac.cn

Introduction

Strong and photostable fluorescence signals are highly desirable for sensitive microarray-based bioanalyses [1]. Nanostructured materials including nanoparticles, nanowires, and nanotubes are able to exhibit extraordinary physical and chemical properties useful for analytical applications [2–9]. The emerging nanotechnology has opened up new exciting avenues for offering great opportunities for sensitive microarray analysis [1, 10, 11]. Although many nanotechnology-based strategies such as resonance light scattering particles [12, 13], fluorescence resonance energy transfer [14], and surface plasmon resonance [15, 16] have been introduced in an effort to improve the detection sensitivity of microarrays, the development of brilliant nanoparticles still holds great promise in microarray at low cost. Luminescent quantum dots are proven to be promising alternatives to organic dyes for fluorescence-based applications [17–19], and can provide stable fluorescent labeling for microarray-based analyses [20]. Nevertheless, there are many concerns over quantum dots toxicity. In the past 20 years, silica nanoparticles were intensively investigated and found applications in materials science, conjugation of biomolecules, catalysis, sensing, and controlled drug delivery [21, 22]. Further, silica shells can act as a stabilizer to limit the effects of outside environmental factors on the inner surface. The encapsulation of fluorescent molecules in silica

particles enable the protection of the dyes from photo-bleaching [23], which increases their photostability and emission quantum yield due to isolation from possible quenchers like molecular oxygen and water, and thereby the fluorescence is constant and can give an accurate measurement [24, 25]. It is also possible to functionalize the surface of fluorescent silica particles to facilitate their conjugation to bioactive molecules like enzymes, proteins, and antibodies [26]. Therefore, the use of fluorophore-doped silica nanoparticles as labeling reagents for DNA detection can provide higher sensitivity than dye molecules because hybridization events are signaled directly when a large amount of fluorophores are attached to the DNA probe. Reverse microemulsion method was first reported to synthesize catalyst of nanostructured complex oxides [27], which was utilized to prepare fluorescent silica nanoparticles in which organic dye molecules were physically doped [25, 28]. However, to date, the fluorophores were doped into silica by weak physical absorption, which has several drawbacks including poor solubility of the dyes in pure silica, migration, leakage, and aggregation of the dyes, resulting in decreasing fluorescent efficiency and variability in the amount of dye molecules entrapped in each nanoparticle [24, 28–30]. Therefore, in order to obtain stable, highly brilliant silica nanoparticles, it is prerequisite to prepare silica nanoparticles with covalently bonded dye molecule.

Our group developed a class of gold–silica, core–shell nanoparticles that are encapsulated with cyanine dyes for labeling in DNA microarray [31]. A sandwich hybridization model was applied to build the microarray, by which the target DNA was hybridized to oligonucleotide probes initially covalently immobilized onto the aldehyde-functionalized glass slide, followed by fluorescent nanoparticle-conjugated DNA, and was attached to the hybridized target DNA via second hybridization [31]. Although the DNA/nanoparticle conjugates hybridization system showed ten times improvement in sensitivity and showed a limit of detection (LOD) of 1 pM complementary DNA (c-DNA) [31], it is still not very good probably due to the relatively low amount of dye-loading in the particle and low efficiency because the signal amplifier of dye-doped nanoparticle is attached to the hybridized target DNA via second hybridization. Moreover, the major limitation of this method is that the probe DNAs were vertically arrayed onto slides (SuperAldehyde slides) by chemical reaction, which is proven to be complicated and time-consuming [31], and therefore, it is difficult for real-world application. Therefore, great efforts should be devoted to prepare a stable high amount of dye-loaded nanoparticle and to establish a platform so that hybridized target DNA can specifically and efficiently be recognized by signaling nanoparticles. To address those issues, in this paper, we report a novel strategy to develop organic-dye-covalently-doped fluorescent nanoparticles,

which enabled sensitive microarray technology. Using reverse microemulsion method and surface modification, we synthesized a streptavidin-functionalized silica nanoparticle covalently embedded with organic dye molecules, which can specifically recognize the biotin-labeled target DNA hybridized to the array via streptavidin–biotin interaction. The target DNA was hybridized with UV cross-linked probe DNA, which was spotted on amine-functionalized glass slide surface [32]. Therefore, it is convenient and easy to implement [32]. Such a system has the following unique characteristics: (a) this strategy is highly advantageous since the synthesis is simple and can be easily scaled up to prepare a large amount of fluorescent particles at relatively low cost; and (b) homogenous, fluorescent nanoparticles specifically recognize biotin-labeled target DNA hybridized to the array via streptavidin–biotin interaction, and this eliminates any background signal interference and greatly improves the detection specificity. This nanotechnology-based approach may allow for the detection of environmental microorganisms more quickly, efficiently, and cost-effectively than those with traditional methods.

Materials and methods

Chemicals and reagents

(3-Aminopropyl)triethoxysilane (APTES), (3-mercaptopropyl)trimethoxysilane (MPTMS), tetraethyl orthosilicate (TEOS) (99.999%), Triton X-100, ammonium hydroxide (28%), bovine serum albumin (BSA), 20× SSC buffers, *n*-hexanol, cyclohexanol, hydrofluoric acid, and acetone were purchased from Sigma-Aldrich Chemical (St. Louis, MO, USA). Streptavidin–maleimide from *Streptomyces avidinii* was obtained from Sigma Chemical (St. Louis, MO, USA). Alexa Fluor® 647 carboxylic acid, succinimidyl ester (AF647-NHS) was obtained from Invitrogen (Carlsbad, CA, USA). All the chemicals are used as received without further purification. DNA oligomers including probe DNA and target DNAs (Table 1) were synthesized by Eurofins MWG Operon (Huntsville, AL, USA).

Preparation of AF647-conjugated APTES precursor

The coupling of AF647 to APTES was carried out in a nitrogen gas-protected cabinet. Briefly, 1.5 ml of anhydrous *n*-hexanol was added in a glass vial. Then, 3.6 μl of anhydrous APTES and 1 mg of AF647-NHS were added under mild stirring. The mixture was continued to stir under darkness. The reaction was stopped after 24 h. The resultant conjugate solution is denoted as AF647–APTES, which was aliquoted into several centrifugal tubes and well wrapped with parafilm, further wrapped with aluminum

Table 1 DNA sequences used in this study

Oligomer name	Sequence(5′→3′)	Description
Probe-I	d(CCG CAC CTC GGA CCG CAC ACA ATC GTT TGA GGA CGT GTA GCT GTG CTG GC)	Universal probe DNA
Target-I	[Cy3]-d(GCC AGC ACA GCT ACA CGT CCT CAA ACG ATT GTG TGC GGT CCG AGG TGC GG TTT TTT TTT TTT TTT)-[BioTEG-Q]	Target DNA containing complementary sequence to the universal probe with 5′ end labeled with Cy3 and 3′ end labeled with biotin
Target-II	[Cy3]-d(*CCG CA*C *CTC* **GGA CCG** C*AC AC*A *ATC GTT TGA* G*GA C*GT G*TA G*C*T GT*G *CTG* GC TTT TTT TTT TTT)-[BioTEG-Q]	Noncomplementary target DNA with 5′ end labeled with Cy3 and 3′ end labeled with biotin

foil, and stored at 4 °C for the following preparation of dye-doped silica nanoparticles.

Synthesis of dye-chemically-doped silica nanoparticles

Briefly, in 50-ml flask, 15 ml of cyclohexanol, 3.54 g of Triton X-100, 3.1 ml of *n*-hexanol, and 0.96 ml of water were mixed well under stirring. Then, 0.5 ml of AF647–APTES in *n*-hexanol was added and stirred for at least 15 min. After that, 140 μl of TEOS was added. The condensation reaction was activated by adding 140 μl of 28% ammonium hydroxide. The reaction was left 18 h under vigorous stirring at room temperature, resulting in chemically AF647-doped silica particles. Finally, additional 80 μl of MPTMS was added, and the reaction was continued to stir for 6 h. A shell of silica coating was generated and tailored with thiol as the functional group. Finally, 7 ml of acetone was added to cease the reaction, and the nanoparticles were isolated by centrifugation and purified by washing with 95% ethanol and water, respectively, each twice to remove any unreacted reagents. The particles were dispersed in acetone and aliquoted into microcentrifuge tubes and dried under vacuum. (To avoid possible photobleaching, all the following experiments including synthesis of dye-doped silica nanoparticles and preparation of nanoparticle–streptavidin conjugates were conducted in the dark by wrapping the reaction tube with aluminum film.) For the measurement of the particle size and dye-loading in the particle, the as-prepared dye-doped silica nanoparticles were resuspended in water at concentration of ~2×10^{13} particle mL^{-1}.

Covalent conjugation of streptavidin onto the fluorescent silica nanoparticle surface

The AF647-doped silica nanoparticle was conjugated to streptavidin by the covalent linkage of streptavidin–maleimide to thiol-bearing fluorescent silica particles. The dye-doped nanoparticle with suitable streptavidin loading can be obtained by changing the ratio of maleimide-labeled streptavidin to thiol-bearing silica and the reaction time.

Characterization of fluorescent silica nanoparticles

UV–Vis–NIR adsorption spectra were measured by using UV–Vis–NIR absorption spectroscopy (Shimadzu, Kyoto, Japan). Fluorescence spectra for the AF647-doped nanoparticles were obtained by using spectrofluorophotometer (RF-5301, Shimadzu, Kyoto, Japan), with the excitation wavelength of 647 nm. FT-IR spectra were taken on a Nexus 470 FT-IR spectrometer (Nicolet, Vernon Hills, IL, USA). The transmission electron micrograph (TEM) images and scanning electron micrograph (SEM) images were obtained using a transmission electron microscope (JEOL2000, 200 kV) and scanning electron microscope (JEOL JSM-880, 15 kV), respectively. The hydrodynamic diameter and size distribution (polydispersity index) of nanoparticles were measured using dynamic light scattering (DLS; Malvern, Autoszer 4700). All DLS measurements were done with a wavelength of 532 nm around 25 °C with an angle detection of 90°.

Construction of DNA microarray, hybridization, and post-hybridization staining

Our group has done pioneering work on functional gene arrays for environmental microbial detection and characterization [33–37]. Very recently, we developed high-throughput functional gene microarray (Geochip 3.0) spotted with universal standard probe [38, 39]. In the present work, we used Geochip 3.0 for the hybridization on which the artificial DNA targets labeled with both Cy3 and biotin at two ends hybridized against this universal standard probe (Table 1). The construction of DNA microarray is schematically shown in Fig. 1. Protocols for environmental DNA hybridization assays developed in this group [34, 37] were used with minor modification. Briefly, the microarray slide with the arrays containing oligonucleotide probes was set in a waterproof Corning hybridization chamber (3×9 cm, Corning Life Science, Big Flats, NY, USA) and covered with coverslip, followed by 40 μL of hybridization solution containing 50% formamide, 5× SSC and 0.1% SDS, then 0.1 mg/ml Salmon
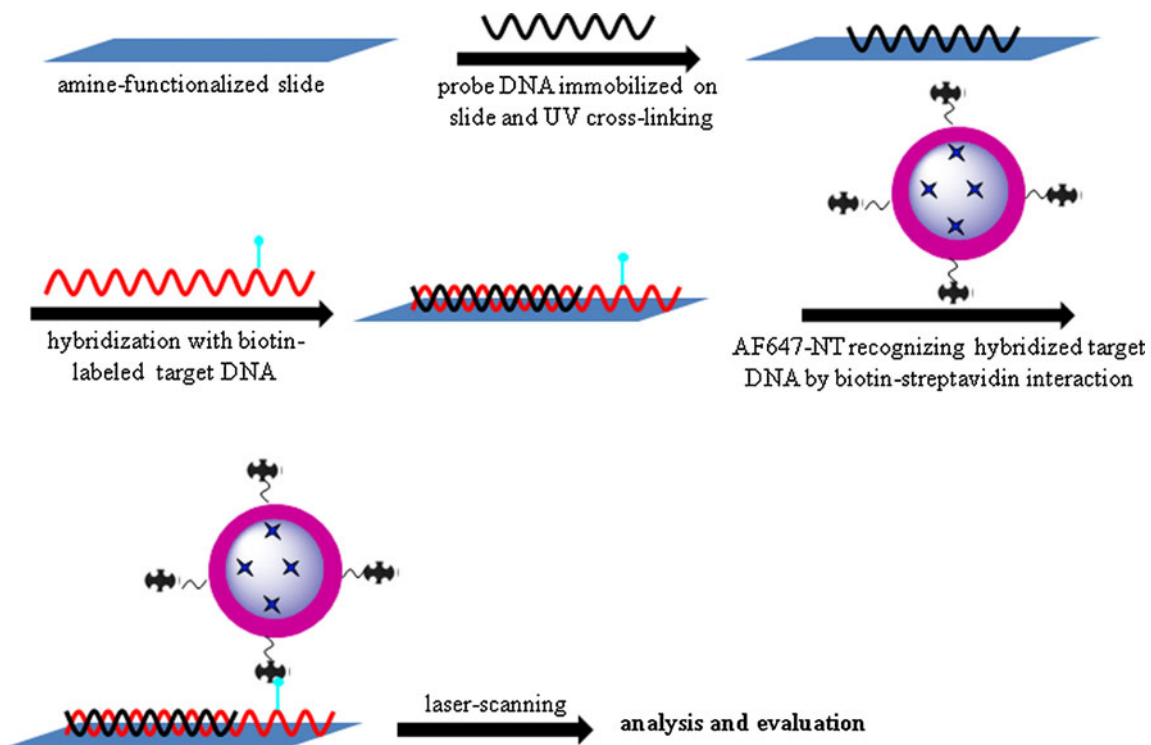
Fig. 1 Schematic construction of DNA microarray

sperm DNA was pipetted along the cross interface between the coverslip and microarray slide; the target DNA solution would spread uniformly on the array area under the coverslip with capillarity. The hybridization was carried out by submerging the hybridization chamber in a 45 °C water bath in the dark for 16 h. After hybridization, the slide with coverslip was immersed in washing buffer I (1× SSC and 0.1% SDS), preheated at 45 °C with the coverslip droping itself in the buffer, then the slides were washed with washing buffer I for 5 min and washing buffer II (0.1× SSC and 0.1% SDS) for 5 min at ambient temperature with gentle shaking. Then, the staining of the hybridized slide was performed by applying 40 μL of the streptavidin-functionalized nano-particle solution prepared with washing buffer I on the DNA-hybridized microarray slides in a similar way as in DNA hybridization. The slide assembly was then shaken in the dark for 40 min at ambient temperature. The chamber was dis-assembled to take the slides, which were washed in washing buffer I for 5 min, in washing buffer II for 5 min, and in 0.1× SSC buffer for 3 min in sequence at ambient temperature; the slides were dried using nitrogen Whoosh duster and were scanned.

Microarray imaging and data analysis

Microarrays were scanned at 10-μm resolution with the scanning laser confocal fluorescence microscope of a ScanArray 5000 system (PerkinElmer LAS, Inc., Shelton,

CT, USA). The emitted fluorescent signal was detected by a photomultiplier tube (PMT) at 570 nm for Cy3 and 670 nm for AF647. The fluorescent signals were analyzed by quantifying the pixel density (intensity) of each spot using ImaGene 6.1 (Biodiscovery, Inc., Los Angeles, CA, USA). The local background signal was automatically subtracted from the hybridization signal of each separate spot, and the mean signal intensity of each spot was used for data analysis. The details for the microarray imaging and data analysis can be found in some papers [34, 40, 41].

Results and discussion

Synthesis and characterization of chemically AF647-doped silica nanoparticles

In the present study, AF647 was used because it exhibits more intense fluorescence due to its higher quantum yield (0.35) than Cy5 and available in a variety of reactive forms. The other reasons are that AF647 and Cy5 have almost identical excitation wavelength and molar extinguishing coefficient. Further, the emission wavelengths for the two dyes are close to each other (670 nm for Cy5 and 655 nm for AF647). Thus, it is not necessary to change the lasers because scanner lasers for Cy3 and Cy5 are already available in this lab.

AF647-silane precursor was initially prepared in the absence of any humidity, which is then involved in the co-

polymerization reaction with TEOS to form silica particles by reverse microemulsion method. The dye-doped particles formed in 12 h and the particle size did not change so much upon further reaction. Here, we kept the reaction for 18 h in order to obtain high dye-loading. The FT-IR spectrum (Supplementary Information Fig. S1A) shows a strong band at 1,652 cm^{-1}, indicating the bond of NH–C=O, which is the evidence of AF647 covalently linked to APTES. The band at 1,107 cm^{-1} is from Si–O–Si vibration, suggesting the fully condensed siloxane center (Fig. S1A). The chemical attachment of dye molecules on the silica backbone did not change the optical properties of the dye. AF647 encapsulated in the silica particles exhibited absorbance peak at 648 nm, which is essentially the same as free AF647 molecules (Fig. 2A, line a). Moreover, the thus-prepared covalently AF647-linked silica particle solution shows higher fluorescence intensity (Fig. 2B, line a), suggesting that the dye-linked APTES conjugate is useful to stabilize the fluorescence. The average number of dye molecules associated with each silica particle was estimated using the following method. A 250-μL of covalently AF647-attached silica nanoparticle solution was treated with diluted hydrofluoric acid to dissolve the nanoparticle so that the dye molecules were released. The resulting mixture was centrifuged, and the fluorescence of the AF647 dyes in the supernatant solution was determined using a fluorospectrometer. The numbers of conjugated dyes per particle were about 125 dye molecules, estimated by dividing the total number of dye molecules by the total number of silica nanoparticles. In order to functionalize the fluorescent particles, thiol group is attached by copolymerization with MPTMS. From FT-IR spectrum, a new peak appeared at 2,935 cm^{-1}, which is the evidence for the C–H vibration from MPTMS (Fig. S1B). Further, a small peak appeared at 2,590 cm^{-1}, which is from R–SH vibrations, suggesting the successful attachment of –SH group (Fig. S1B). This is also evidenced by the energy dispersive spectrum of the prepared particle, from which a small peak for sulfur was clearly observed (Supplementary Information Fig. S2). The particles were uniform in size (Fig. 3). From DLS measurement, the average size of the particles is 49± 3 nm. It is interesting to note that the UV–Visible spectrum and fluorescence spectrum for thiol-functionalized fluorescent nanoparticle are essentially the same as that prior to thiol-functionalization (line b in Fig. 2A, B), suggesting that the surface modification could not change the optical properties of the entrapped dye molecules. The prepared silica nanoparticle solution was kept for 1 week, followed by centrifugation to collect the pellets, and redispersed in the same volume of buffer solution, whose fluorescence intensity was unchanged after measurement, suggesting that the dye molecules are well linked to the silica particles.

Functionalization of fluorescent silica nanoparticle

We functionalized silica particle surface with streptavidin molecules. This is because streptavidin is a glycoprotein and known to contain four identical binding sites to biotin with a binding constant of ca. 10^{14} M^{-1} [42]. Actually, streptavidin–biotin interaction was used to study single-nucleotide polymorphism analysis using fluorescence resonance energy transfer between DNA-labeling fluorophore [43]. Streptavidin–maleimide was used because maleimide/–SH interaction is highly specific, efficient, and therefore can result in a stable thioether linkage. Covalent coupling of maleimide-activated streptavidin to thiol-bearing nanoparticle is performed in PBS buffer (25 mM sodium phosphate containing 25 mM sodium chloride, pH 7). We tested different ratios of maleimide-activated streptavidin to thiol-bearing nanoparticle and found that a ratio of 8:1 is good for the linkage. The reaction is done overnight with gentle stirring at room temperature. The resultant streptavidin-attached fluorescent particle is 54±4 nm in size with polydispersity index of 0.13 from DLS measurement, suggesting the monodispersity of the modified particles.

Fig. 2 (A) Typical UV–visible spectra for covalently AF647-doped silica nanoparticles prior to (a) and after thiol functionalization on the surface (b). (B) Fluorescence emission spectra of covalently AF647-doped silica nanoparticle before condensation with MPTMS (a) and after condensation with MPTMS for 6 h (b). Excitation wavelength, 647 nm
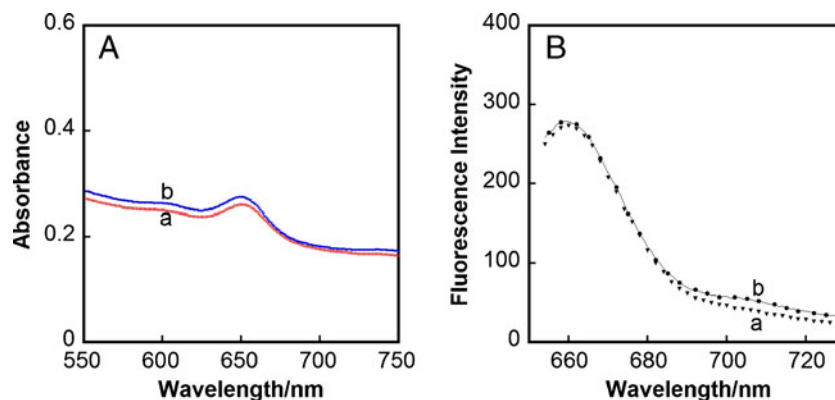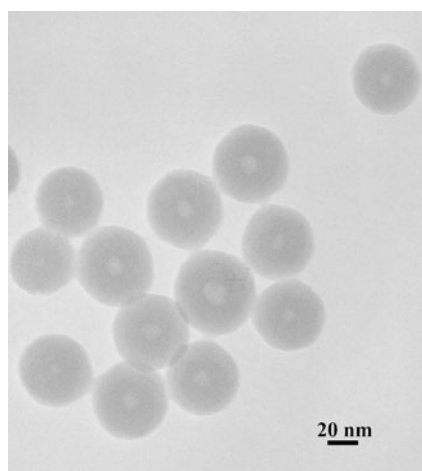
Fig. 3 TEM images of surface thiol-functionalized fluorescent silica nanoparticles

Eliminating background signal interference from the fluorescent particle by coating with BSA

Background signal is generally large in biochip assays if any molecules are adsorbed on a slide surface. In a preliminary experiment, the thus-prepared streptavidin-attached fluorescent particle showed strong adsorption towards the slide surface, resulting in high background intensity ranging from 4,300 to 18,000 (70% laser power and 60% PMT gain). In order to overcome this, we mixed the fluorescent silica nanoparticle solution with 1% BSA solution prepared with washing buffer I under gentle shaking for 2 h, followed by washing. Two hundred fifty microliters of BSA-treated nanoparticle was spotted on the slide surface, washed, and dried. The resultant slide showed a background intensity ranging from 140 to 240 (70% laser power and 60% PMT gain). That is, the BSA-modified fluorescent nanoparticle showed negligible nonspecific adsorption on the slide surface. The minimum of nonspecific adsorption of the BSA-covered streptavidin–fluorescent nanoparticles on the slide surface proved the effective blocking of the silica nanoparticle surface. Therefore, in the following experiment, the BSA-coated streptavidin–fluorescent nanoparticle (AF647–NT) solution was used as signaling probe to stain hybridized target DNA. The SEM image for the BSA-adsorbed nanoparticle is shown in Fig. S3. The particle has the size of 54±3 nm, and the size distribution is 0.12 from DLS measurement. Therefore, the BSA-modified particles are monodisperse.

DNA microarray stained with streptavidin–fluorescent nanoparticle

The possibility of using AF647–NP as labeling for microarray technology was explored, by which a functional gene microarray (Geochip 3.0) with an universal probe (50-mer)

developed in our group was used. The DNA sequence of the universal probe is listed in Table 1. The universal probe DNA was co-immobilized with each functional gene probes on the amine-functionalized slides to fabricate an oligonucleotide microarray with UV cross-linking (Fig. 1). Two of 65-mer oligonucleotides (one containing the complementary sequence to the universal probe and another containing mismatched sequence) were used as target DNAs (Table 1). In order to compare the hybridization sensitivity of the AF647–NP staining with that of traditional labeling and hybridization, the 3′ end of the target DNAs was initially labeled with Cy3. After hybridization, the staining of the microarray with the AF647–NP conjugate was followed. The hybridization and staining procedures are schematically demonstrated in Fig. 1. The obtained two-color hybridization microarray images are shown in Fig. 4, in which the left
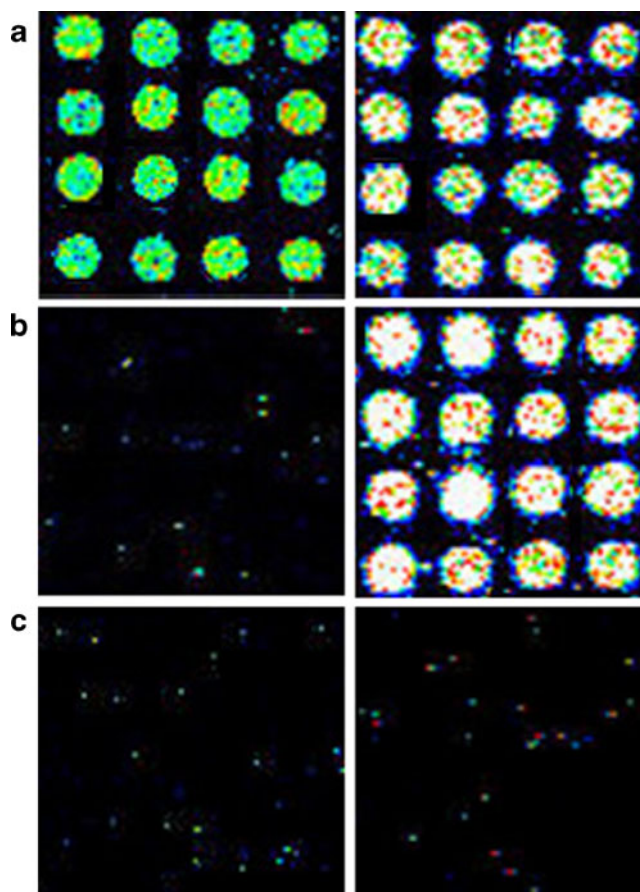

Fig. 4 Two-color microarray images. The probe-I-spotted slide was hybridized with target-I DNA at different concentrations. After washing, the microarray was stained with the same amount of AF647–NP solution. Hybridization images were scanned after the slides were washed as described in the text. The images on the *left side* and *right side* were scanned at Cy3 channel and Cy5 channel, respectively. (a) Target-I DNA, 1.54 nM; PMT gain (70%); and laser power (70%). (b) Target-I DNA, 100 pM; PMT gain (85%); and laser power (85%). (c) Target-II DNA, 100 pM; PMT gain (85%); and laser power (85%)

panels are for Cy3 and the right ones are for AF647–NT. The slide stained with AF647–NT after hybridization showed negligible nonspecific adsorption in the universal DNA probes that immobilized on the slide surface (Fig. 4b). When the Cy3 (570 nm) and Cy5 (670 nm) channels were scanned under low laser power, the spots on the microarray which hybridized with nanomolar c-DNA were clearly observed for Cy3 and AF647–NT. However, the spots for AF647–NT are about 40-fold brighter (Fig. 4a). With the use of a higher laser power and PTM gain, the fluorescence signal of the spots for AF647–NT are almost saturated (Fig. 4a). Therefore, the contrast was not so obvious. The contrast should be sharp if much lower laser power and PMT gain were used. On the other hand, although both the laser power and PMT gain were increased, for 100 pM c-DNA (target-I), the spot image for Cy3 was un-distinguishable, and the spots for AF647–NT were still very brilliant (Fig. 4b). It should be noted here that for each c-DNA concentration, the laser power and PMT gain for Cy3 and AF647–NT were set the same. No signals were observed for noncomplementary target-II at different concentrations (Fig. 4c). These results suggest that the AF647–NP can be used as the signaling agents in detection of DNA hybridization. There are scatterings for AF647–NP stained spots from the microarray image, which were probably originating from non-shaking during the manual hybridization chamber and the inconsistent shaking during washing step. This phenomenon should be greatly improved by using hybridization station with slidewasher.

The photostability of the microarray signal was compared by continuously scanning the DNA microarray slides that employed AF647-doped nanoparticles or AF647 fluorophore as the label under laser power of 85% and PMT gain of 85%. The signal intensity of the microarrays with AF647-doped nanoparticles decreased to 95% of their initial intensities after ten continuous scans. However, the signal intensity of the microarrays with pure AF647 as the label dropped to 72%. These results showed that AF647 dye embedded in the nanoparticles were more photostable than the conventional AF647 label. Therefore, the higher photostability of the fluorescent nanoparticles made the assay more reproducible and accurate.

The sensitivity using AF647–NP as labeling agent in microarray technology was investigated. In all cases, 40 μl of AF647–NP solution was applied in the post-hybridization experiments. The signal intensity as a function of the c-DNA concentration was plotted by performing the hybridization with target-I at different concentrations (Fig. 5). The shape of the curve is sigmoid and has a linear range between 0.2 and 10 pM c-DNA. The LOD is found to be 0.1 pM (signal-to-noise ratio of 3). Recent papers reported DNA microarrays capable of picomolar DNA determination based on enzyme-induced deposition of silver nanoparticles (LOD, 5 pM) [32], gold
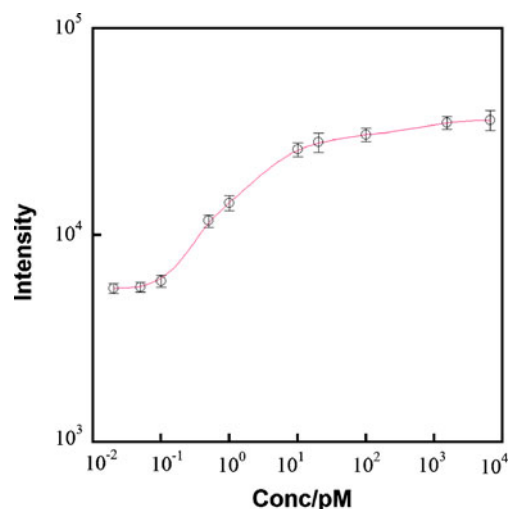

Fig. 5 Response–dose curve for target-I DNA. The fluorescent signal was obtained by scanning the slides at Cy5 channel with PMT gain (85%) and laser power (85%)

nanoparticle labeling method (LOD, 1 pM) [44, 45], dye-doped, gold–silica, core–shell nanoparticles (LOD, 1 pM) [31], chip-based microbead arrays (LOD, 0.1 pM) [46], and luminescent nanoparticles as probes (LOD, 0.05 pM) [47]. Obviously, our LOD value by using the fluorescent chemically embedded AF647–NP is competitive with the best values previously reported for DNA microarrays using other fluorescent nanoparticles as labeling.

Detection of pure culture DNA using AF647–NP staining

To test whether the AF647–NP staining approach can be used for real DNA microarray hybridization, pure DvH genomic DNA and DvH whole genome oligonu-
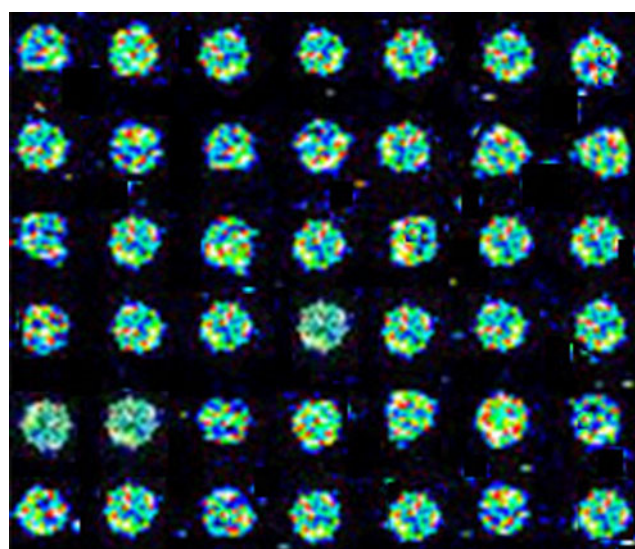
Fig. 6 Microarray image for 100 ng biotin-labeled DvH DNA hybridized after stained with AF647–NP

cleotide microarray were used. The DvH DNA was labeled with biotin using NEBlot® phototope® kit from New England Biolab (NEB, MA) (http://www.neb.com/nebecomm/products_intl/productN7550.asp), followed by purification with QIAquick PCR purification column. After hybridization with DvH array, the slide was stained with AF647–NP. Usually, 500 ng DvH DNA was used in our traditional DvH whole genome oligonucleotide microarray-based assay. In the microarray image shown in Fig. 6, however, 100 ng DvH DNA in the hybridization buffer solution gave similar hybridization signal as 10 pM artificial target was used in hybridization to the universal probe. Therefore, the use of post-hybridization secondary detection approach is feasible in the application to sensitive microarray hybridization technology.

Conclusions

We developed a novel class of streptavidin-functionalized silica nanoparticles with cyanine dye molecules were chemically doped. The resultant nanoparticles are highly fluorescent and photostable, and especially exhibit strong specific interaction with biotin-linked DNAs. Therefore, the use of streptavidin-functionalized fluorescent silica nanoparticles as the detecting reagents in DNA microarray hybridization can be realized. We also demonstrated that after surface modification with BSA, the reactant nanoparticle exhibited negligible nonspecific background signal. The enhancement of DNA detection sensitivity was achieved by using this novel fluorescent nanoparticle as detecting reagents in microarray hybridization. This approach has been successfully applied to pure culture genomic DNA microarray hybridization, and may be potentially applied to other binding events such as specific interactions between proteins. Further experiments are necessary to optimize this DNA microarray technology aiming at the sensitive detection of microbial organisms from environmental samples, such as from groundwater, soil, sediments, contaminated sites, oil fields, animal guts, and for clinical use.

References

1. Lytton-Jean AKR, Han MS, Mirkin CA (2007) Anal Chem 79:6037–6041
2. Curreli M, Li C, Sun Y, Lei B, Gundersen MA, Thompson ME, Zhou C (2005) J Am Chem Soc 127:6922–6923
3. Liu A, Wei M, Honma I, Zhou H (2005) Anal Chem 77:8068–8074
4. Patolsky F, Zheng G, Lieber CM (2006) Anal Chem 78:4260–4269
5. Liu A, Wei MD, Honma I, Zhou H (2006) Adv Funct Mater 16:371–376
6. Liu A, Honma I, Zhou H (2007) Biosens Bioelectron 23:74–80
7. Liu A, Zhou H, Honma I, Ichihara M (2007) Appl Phys Lett 90:253112
8. Liu A (2008) Biosens Bioelectron 24:167–177
9. Stern E, Klemic JF, Routenberg DA, Wyrembak PN, Turner-Evans DB, Hamilton AD, LaVan DA, Fahmy TM, Reed MA (2007) Nature 445:519–522
10. Chen Z, Tabakman SM, Goodwin AP, Kattah MG, Daranciang D, Wang X, Zhang G, Li X, Liu Z, Utz PJ, Jiang K, Fan S, Dai H (2008) Nat Biotech 26:1285–1292
11. Algar WR, Massey M, Krull UJ (2009) Trends Analyt Chem 28:292–306
12. Bao P, Frutos AG, Greef C, Lahiri J, Muller U, Peterson TC, Warden L, Xie X (2002) Anal Chem 74:1792–1797
13. Piao JY, Park EH, Choi K, Quan B, Kang DH, Park PY, Kim DS, Chung DS (2009) Analyst 80:967–973
14. Zhang S, Metelev V, Tabatadze D, Zamecnik PC, Bogdanov A (2008) Proc Natl Acad Sci USA 105:4156–4161
15. Fang S, Lee HJ, Wark AW, Corn RM (2006) J Am Chem Soc 128:14044–14046
16. Cooper MA (2002) Nat Rev Drug Discov 1:515–528
17. Chan WCW, Nie S (1998) Science 281:2016–2018
18. Jaiswal JK, Mattoussi H, Mauro JM, Simon SM (2003) Nat Biotechnol 21:47–51
19. Gerion D, Parak WJ, Williams SC, Zanchet D, Micheel CM, Alivisatos AP (2002) J Am Chem Soc 124:7070–7074
20. Gerion D, Chen F, Kannan B, Fu A, Parak W, Chen D, Majumdar A, Alivisatos A (2003) Anal Chem 75:4766–4772
21. Burns A, Ow H, Wiesner U (2006) Chem Soc Rev 35:1028–1042
22. Bagwe RP, Hilliard LR, Tan W (2006) Langmuir 22:4357–4362
23. Kim HK, Kang SJ, Choi SK, Min YH, Yoon CS (1999) Chem Mater 11:779–788
24. Zhao X, Tapec-Dytioco R, Tan W (2003) J Am Chem Soc 125:11474–11475
25. Zhao X, Bagwe RP, Tan W (2004) Adv Mater 16:173–176
26. Rossi LM, Shi L, Rosenzweig N, Rosenzweig Z (2006) Biosens Bioelectron 21:1900–1906
27. Zarur AJ, Ying JY (2000) Nature 403:65–67
28. Tapec R, Zhao XJ, Tan W (2002) J Nanosci Nanotech 2:405–409
29. Yong K-T, Roy I, Swihart MT, Prasad PN (2009) J Mater Chem 19:4655–4672
30. Bonacchi S, Genovese D, Juris R, Montalti M, Prodi L, Rampazzo E, Zaccheroni N (2011) Angew Chem Intl Ed 50:4056–4066
31. Zhou X, Zhou J (2004) Anal Chem 76:5302–5312
32. Schüler T, Nykytenko A, Csaki A, Möller R, Fritzsche W, Popp J (2009) Anal Bioanal Chem 395:1097–1105
33. Wu L, Thompson DK, Li G, Hurt RA, Tiedje JM, Zhou J (2001) Appl Environ Microbiol 67:5780–5790
34. He Z, Wu L, Fields MW, Zhou J (2005) Appl Environ Microbiol 71:5154–5162
35. Zhou J, Kang S, Schadt CW, Garten CT (2008) Proc Natl Acad Sci USA 105:7768–7773
36. Zhou J (2009) Phytopathol 99:S164–S164
37. He Z, Gentry TJ, Schadt CW, Wu L, Liebich J, Chong SC, Wu WM, Gu B, Jardine P, Criddle C, Zhou J (2007) ISME J 1:67–77
38. He Z, Deng Y, Van Nostrand JD, Tu Q, Xu M, Hemme CL, Li X, Wu L, Gentry TJ, Yin Y, Liebich J, Hazen TC, Zhou J (2010) ISME J 4:1167–1179
39. Liang Y, He Z, Wu L, Deng Y, Li G, Zhou J (2010) Appl Environ Microbiol 76:1088–1094
40. Liebich J, Chong SC, Schadt C, He Z, Zhou J (2006) Appl Environ Microbiol 72:1688–1691

41. Wang X, Gao H, Shen Y, Weinstock GM, Zhou J, Palzkill T (2008) Nucleic Acids Res 36:4863–4871
42. Hsu S-M (1990) In: Wilchek M, Bayer EA (eds) Avidin-biotin technology: methods in enzymology, vol 184. Academic, San Diego, pp 357–363
43. Nakayama H, Arakaki A, Maruyama K, Takeyama H, Matsunaga T (2004) Biotechnol Bioeng 84:96–102
44. Park S-J, Taton TA, Mirkin CA (2002) Science 295:1503–1506
45. Kim H, Takei H, Yasuda K (2010) Sens Actuators B Chem 144:6–10
46. Ali MF, Kirby R, Goodey AP, Rodriguez MD, Ellington AD, Neikirk DP, McDevitt JT (2003) Anal Chem 75:4732–4739
47. Wang L, Lofton C, Popp M, Tan W (2007) Bioconjugate Chem 18:610–613